ELSEVIER

Journal of Magnetism and Magnetic Materials 191 (1999) 331–338

Journal of magnetism and magnetic materials

# Magnetic properties of epitaxial $Fe(Si_{1-x}Fe_x)$ films grown on Si(1 1 1)

D. Berling[a], G. Gewinner[a], M.C. Hanf[a,*], K. Hricovini[b,c], S. Hong[a], B. Loegel[a], A. Mehdaoui[a], C. Pirri[a], M.H. Tuilier[a], P. Wetzel[a]

[a]*Laboratoire de Physique et de Spectroscopie Electronique, UPRES. A 7014, 4 rue des Frères Lumière, 68093 Mulhouse Cedex, France*
[b]*Laboratoire pour l'Utilisation du Rayonnement Electromagnétique, Université Paris-Sud, 91405 Orsay, France*
[c]*LPMS, Université de Cergy-Pontoise, Neuville-sur-Oise, 95031 Cergy-Pontoise, France*

Received 8 June 1998; received in revised form 7 September 1998

**Abstract**

Iron silicide thin films (200 Å $Fe(Si_{1-x}Fe_x)$ with $0 \leqslant x \leqslant 1$ and local cubic CsCl structure) have been grown by coevaporation at room temperature (RT) on Si(1 1 1). X-ray magnetic circular dichroism (XMCD) and magneto-optic Kerr effect (MOKE) measurements indicate that the films are ferromagnetic at RT for $x$ ranging from 1 (pure Fe) to 0.15 ($Fe_{1.35}Si$). The magnetization is parallel to the film surface, and the magnetic anisotropy is uniaxial, with the easy axis lying along a $[\bar{1}\,0\,1]_{Si}$ crystallographic direction and the hard axis along a $[1\,\bar{2}\,1]_{Si}$ direction of the substrate. MOKE measurements show that the magnitude of the saturation field increases with increasing Si concentration, while XMCD data indicate that the average local magnetic moment carried by the Fe atoms decreases with decreasing Fe concentration. Models which involve the diminution of the number of Fe nearest neighbors are proposed for the description of the behavior of the Fe moments. 

*PACS:* 75.70.Cn; 78.70.Dm; 75.25. + z; 75.50.Bb; 75.30.Gw

*Keywords:* Iron silicide; X-ray magnetic circular dichroism; Film growth; Kerr effect; Ferromagnetism

## 1. Introduction

Fe silicides have been widely studied in the past years for their fundamental aspect as well as for possible applications in microelectronics. Bulk $Fe(Si_{1-x}Fe_x)$ forms a continuous range of solid solutions with a cubic structure between $x = 0.46$ ($Fe_{2.7}Si$) and 1 (pure Fe) [1]. However Si-rich silicides, that do not exist in the bulk form, can be stabilized as thin layers. Indeed $Fe(Si_{1-x}Fe_x)$ layers with $0 \leqslant x \leqslant 1$ can be grown pseudomorphically in the whole composition range on Si(1 1 1) by coevaporation of Si and Fe at room temperature (RT) [2]. Now the bulk cubic Fe–Si alloys ($0.46 \leqslant x \leqslant 1$) are known to be ferromagnetic, with a Curie temperature of 830 K for $Fe_3Si$ [3]. Thus the possible

* Corresponding author. Tel.: 33-3-89-33-64-36; fax: 33-3-89-33-60-83; e-mail: m.hanf@univ-mulhouse.fr.

0304-8853/99/$ – see front matter 
PII: S0304-8853(98)00369-2

ferromagnetic character of the films would allow the integration of magnetic devices in silicon technology.

In this paper we show by means of the magneto-optic Kerr effect technique (MOKE) and X-ray magnetic circular dichroism (XMCD) that $Fe_3Si$ films, like bulk $Fe_3Si$, are ferromagnetic at RT, and for the first time it is shown that silicide films for $0.15 \leqslant x \leqslant 0.5$ are ferromagnetic as well. In particular, we show that the magnetic moment carried by the Fe atoms decreases steadily with decreasing Fe concentration and vanishes for FeSi (CsCl, $x = 0$). Different models are proposed to describe the variation of the magnetic moment with Fe content.

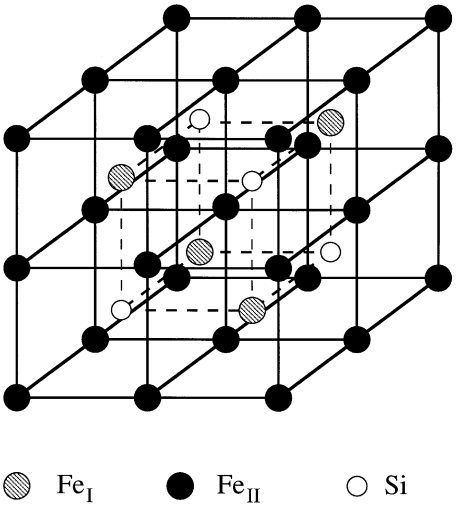


Fig. 1. Unit cell of the $DO_3$-type $Fe_3Si$ structure. The $Fe_I$ are surrounded by eight $Fe_{II}$, and the $Fe_{II}$ are surrounded by four $Fe_I$ and four Si.

## 2. Experiment

The films have been grown in ultra high vacuum (UHV) by the coevaporation of Fe and Si on the substrate kept at RT. The substrate was made of a 10 Å thick codeposited FeSi template layer initially grown on Si(1 1 1). This completely avoids the interdiffusion with the Si substrate that takes place even at RT for the Fe-rich films and considerably improves the structural quality of the layers. Indeed such films, whose thickness was $\sim$200 Å, exhibited good $(1 \times 1)$ LEED and IMEED patterns indicating the epitaxy of the silicides [2]. In the same manner 200 Å BCC Fe has been grown epitaxially as a reference. Finally, all the films were capped with a 20 Å Si layer to protect them from oxidation before they were removed from the UHV chamber. More details about sample preparation and structural characterization can be found in Ref. [2].

All the films are metallic and present a cubic structure that can be derived from the $DO_3$ type structure of $Fe_3Si$. This structure, displayed in Fig. 1, may be viewed as a CsCl-type lattice made of two simple cubic sublattices. The sites of one sublattice are occupied by Fe atoms only ($Fe_{II}$ in Fig. 1), while the other sublattice is made of 50% Si and 50% Fe ($Fe_I$ in Fig. 1). In bulk $Fe_3Si$, long range crystallographic order is present: $Fe_I$ atoms have eight $Fe_{II}$ nearest neighbors (NN), and six Si next nearest neighbors (NNN), while Si atoms have eight $Fe_{II}$ NN, and six $Fe_I$ NNN. In the deposited films however, only local $DO_3$ order is observed by X-ray photoelectron diffraction, as no superstructure was revealed by X-ray diffraction [4]. Local $DO_3$ order means that one sublattice is actually occupied with Fe atoms only, while 50% Fe and 50% Si atoms are randomly located on the second. For Fe-rich silicides (from $Fe_3Si$ to pure Fe, $0.5 \leqslant x \leqslant 1$), Fe atoms substitute Si atoms in $DO_3$-type $Fe_3Si$. For films poorer in Fe than $Fe_3Si$ ($0 \leqslant x \leqslant 0.5$), the $Fe_I$ atoms are replaced by Si atoms. As $x$ represents the Fe concentration on the second sublattice containing both Fe and Si species, for $x = 0$, there are no $Fe_I$ any more. This corresponds to the metastable FeSi(CsCl) cubic silicide, where Fe atoms have eight Si NN and six Fe NNN [5,6]. From now on, the denomination FeSi will refer to the epitaxially stabilized FeSi (CsCl) phase grown on Si(1 1 1).

The magnetic properties of the samples were characterized by ex situ MOKE at RT. The MOKE system consists of a polarized laser source, two polarizers, a photo-elastic modulator and a photodiode detector. Measurements were performed in the longitudinal geometry, i.e. with the magnetic field applied in the sample plane and in the plane of incidence. The incidence of the light was $\sim 45^\circ$ with respect to the sample surface normal.

The XMCD measurements have been performed at the Laboratoire pour l'Utilistation du Rayonnement Electromagnétique (LURE) on the SU 23 beam line of the Super ACO storage ring using circularly polarized light. The rate of circular polarization was $\sim 70\%$. The samples have been analyzed in remanence at RT by absorption at the Fe $L_{2,3}$ edges. The incidence of the light was $60^\circ$ with respect to the sample surface normal. Dichroism measurements were performed with a constant incident photon spin direction and by reversing the magnetization by means of a magnetic field. The latter was applied parallel to the sample surface and along a $[\bar{1}\,0\,1]_{Si}$ crystallographic direction of the substrate, which, according to the MOKE results that will be shown below, corresponds to the magnetic easy axis direction.

## 3. Results and discussion

Fig. 2a and Fig. 2b display the Kerr loops for four samples ($x = 1$: pure Fe; $x = 0.5$: $Fe_3Si$; $x = 0.33$: $Fe_2Si$; $x = 0.15$: $Fe_{1.35}Si$) recorded with the magnetic field oriented along two perpendicular crystallographic directions, namely $[1\,\bar{2}\,1]_{Si}$ and $[\bar{1}\,0\,1]_{Si}$ respectively. The dashed curve in Fig. 2b for pure Fe is an enlarged view of the curve presented in Fig. 2a. The presence of hysteresis cycles indicates that the films are ferromagnetic at RT for $0.15 \leqslant x \leqslant 1$. No ferromagnetism is observed for $x \leqslant 0.09$, i.e. for iron silicides poorer in Fe than $Fe_{1.35}Si$. The clearcut square loops obtained along $[\bar{1}\,0\,1]_{Si}$ indicate that this direction corresponds to a magnetic easy axis, whatever the value of the Fe concentration. This shows that all silicide domains have the same easy axis. Fig. 2a

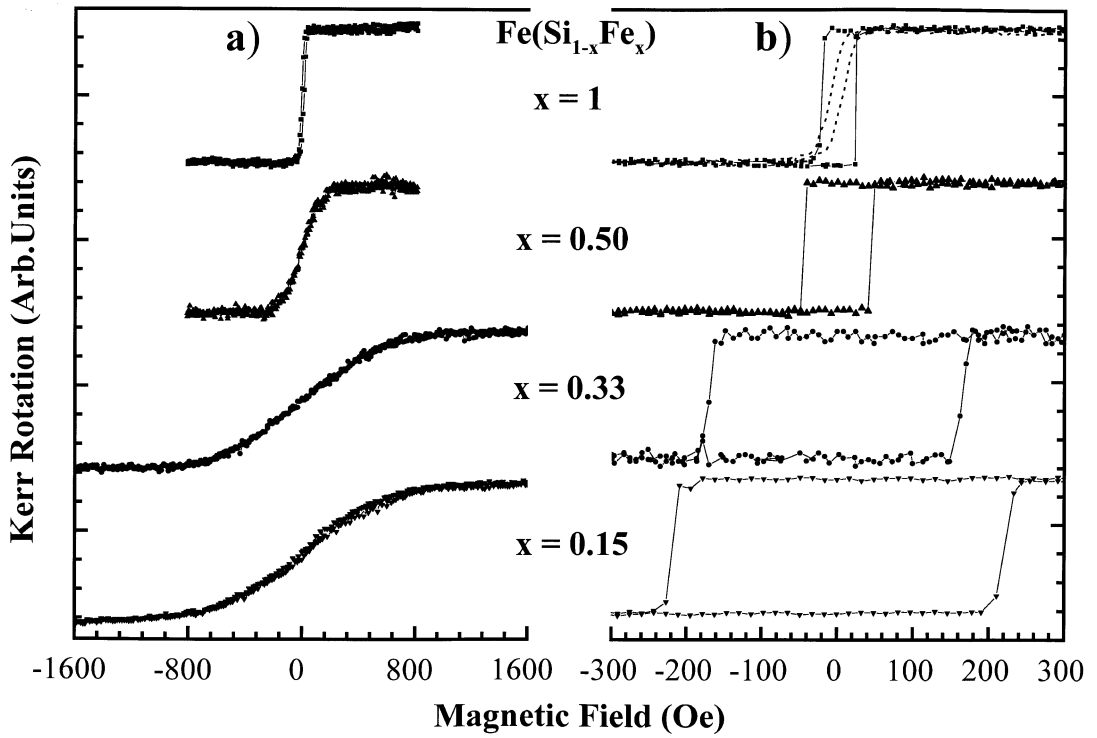


Fig. 2. Kerr loops for $x = 1, 0.5, 0.33$, and 0.15 with the magnetic field applied along the $[1\,\bar{2}\,1]_{Si}$ direction (a) and the $[1\,0\,\bar{1}]_{Si}$ direction (b), except for the dashed curve ($x = 1$) which has been recorded with the field along $[1\,\bar{2}\,1]_{Si}$.

also shows a magnetic hard axis, at 90° from the easy axis, along the $[1\,\bar{2}\,1]_{Si}$ direction. Thus we observe for the silicides an in-plane uniaxial magnetic anisotropy, although the surface presents a threefold crystallographic symmetry [4,7]. Similar uniaxial magnetic anisotropy has been already observed for Fe layers deposited on semiconductors but its origin is not well understood [8,22]. It may be related for instance to the direction of the atomic flux during Fe and Si evaporation with respect to the sample axis, or to the strain applied to the substrate by the sample holder during film growth. Concerning the pure Fe layer, the shape of the dashed curve in Fig. 2b recorded along the $[1\,\bar{2}\,1]_{Si}$ direction indicates that, in contrast to the results obtained on the iron silicides layers, this axis is not a real hard axis. In other words, the anisotropy is not uniaxial for the deposited Fe film. Experiments are on the way to clarify these different points.

Table 1 displays the values of the magnetic field $H_{sat}$ at which saturation occurs as a function of $x$ for various ferromagnetic samples. Clearly $H_{sat}$ increases with increasing Si content. Apparently the displacement of the domain walls becomes more and more difficult when the Fe content decreases, probably because of an increasing number of defects. This trend is similar to that observed on bulk alloys of Fe with various elements [9]. Also presented in Table 1 are the anisotropy constants $K$ calculated by minimizing the Zeeman energy when $H$ is applied along the hard axis direction, which leads to

$$K = \tfrac{1}{2}HM,$$

where $H$ is the applied magnetic field and $M$ the magnetization per atom. $M$ is inferred from the XMCD measurements presented in the following paragraph. One observes that $K$ increases very slowly with Si concentration. Note that $K$ is calculated for the silicides only, as for the Fe layer the $[1\,\bar{2}\,1]$ direction is not a magnetic hard axis.

MOKE measurements have shown the ferromagnetic character of the Fe silicide films even for composition very close to FeSi, and the presence of an easy axis parallel to the sample surface and along a $[\bar{1}\,0\,1]_{Si}$ crystallographic direction with a twofold rotational symmetry instead of a threefold one expected from crystallographic crystal symmetry. Furthermore, the square-shaped loops along with a strong $H_{sat}$ dependence with $x$ show that these silicides essentially crystallize in a simple phase with defined composition. The relationship between magnetization and film composition has been investigated by dichroism absorption measurements performed on five samples, namely FeSi ($x = 0$), $Fe_{1.6}Si$ ($x = 0.23$), $Fe_2Si$ ($x = 0.33$), $Fe_3Si$ ($x = 0.5$), and pure BCC Fe ($x = 1$).

Fig. 3 displays the Fe $L_{2,3}$ edge X-ray absorption spectra of $Fe(Si_{1-x}Fe_x)$ layers recorded at RT versus $x$. The data have been normalized to the incident photon intensity. For each concentration two curves, labeled $\sigma_+$ and $\sigma_-$, are presented which are recorded after the magnetic field has been applied in two opposite directions along the magnetic easy axis $[\bar{1}\,0\,1]_{Si}$. Clearly there is a dichroic signal for all samples with $x > 0$, which confirms the ferromagnetic nature of these compounds. No dichroism is detectable for FeSi, in agreement with MOKE measurements.

Fig. 4 presents the differential absorption curves $\sigma_M = (\sigma_+ - \sigma_-)$ for various Fe concentrations. These curves have been normalized to the Fe content of each sample by dividing them by $I(L_3)$,

Table 1
Magnitude of the saturation field $H_{sat}$ as a function of $x$ with the magnetic field applied along the $[\bar{1}\,0\,1]_{Si}$ (easy axis) and $[1\,\bar{2}\,1]_{Si}$ (hard axis) directions. The magnitude of the anisotropy constant for the Fe–Si compounds is also presented (in J/atom)

| | Fe | $Fe_3Si$ | $Fe_3Si$ | $Fe_{1.35}Si$ |
|---|---|---|---|---|
| $x$ | 1 | 0.5 | 0.33 | 0.15 |
| $H_{sat}$ along the easy axis (Oe) | 13 | 78 | 164 | 220 |
| $H_{sat}$ along the hard axis (Oe) | 19 | 173 | 595 | 830 |
| Anisotropy constant (J/at) | | $1.35 \times 10^{-25}$ | $1.6 \times 10^{-25}$ | $2.03 \times 10^{-25}$ |

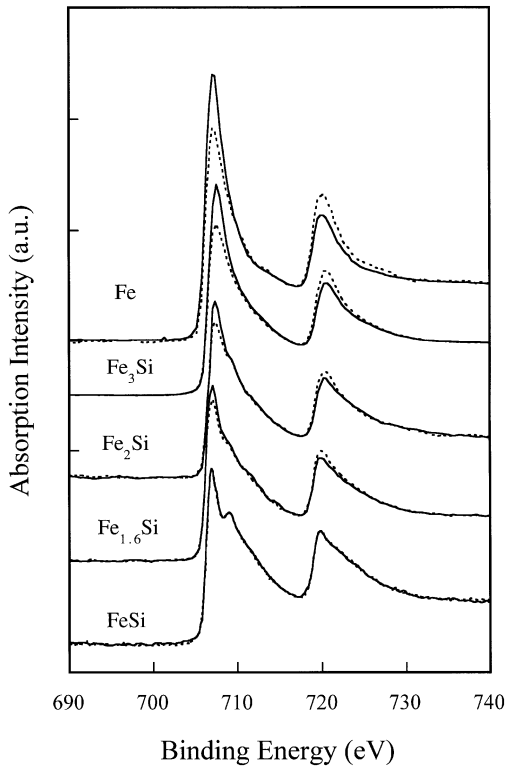


Fig. 3. Fe $L_{2,3}$ X-ray absorption spectra recorded with the magnetic field applied in the two opposite directions [1 0 $\bar{1}$] and [$\bar{1}$ 0 1]. The dashed and solid lines correspond to the $\sigma^+$ and $\sigma^-$ curves, respectively.

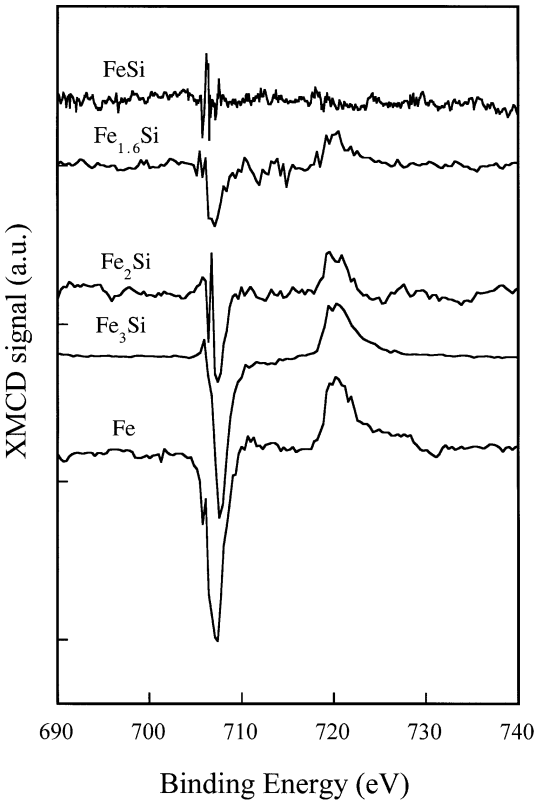


Fig. 4. XMCD signal for various values of $x$. The raw data have been normalized to the Fe content of the samples.

where $I(L_3)$ is the $L_3$ peak area of the half sum of the two $L_3$ peaks taken with both polarizations, namely $(\sigma_+ + \sigma_-)/2$. Here the half summation $(\sigma_+ + \sigma_-)/2$ is assumed identical to the linear polarization absorption spectrum [10]. The statistics becomes poorer as the Fe content diminishes, however it can be clearly seen in Fig. 4 that the dichroic signal intensity decreases when the film is richer in Si, and vanishes for FeSi composition.

In order to get an idea of the magnitude of the average magnetic moment $\mu(x)$ carried by the Fe atoms, we used results obtained by Alouani et al. [11]. They found that the intensity of the calculated dichroic signal for Fe, $Fe_3N$ and $Fe_4N$ compounds is proportional to the spin magnetic moment at the iron site. As the orbital moment is much lower than the spin moment for pure Fe ($\mu_{orb} = 0.046\ \mu_B$, $\mu_{spin} = 2.16\ \mu_B$ [11]), we assumed that the XMCD signal integrated over the $L_3$ part of the $L_{2,3}$ spin–orbit split edge is actually proportional to the average magnetic moment $\mu(x)$. In doing so (we consider $\mu_{orb} \ll \mu_{spin}$ for the whole range of iron silicides) the error is $\sim 2\%$ for pure Fe, which is much smaller than the dispersion of our experimental results. As we are interested in trends only and not in the exact value of the magnetic moment, the different hypothesis and assumptions done are quite reasonable. We proceeded in the following way: first we integrated the normalized XMCD signal over the $L_3$ feature. Then we estimated the Fe average moment $\mu(x)$ for the various samples by considering that it is proportional to the XMCD $L_3$ area, and that its value is 2.22 $\mu_B$ for the pure Fe layer (which corresponds to the bulk BCC Fe value). Indeed for the Fe thickness considered here the film has reached bulk properties as far as the

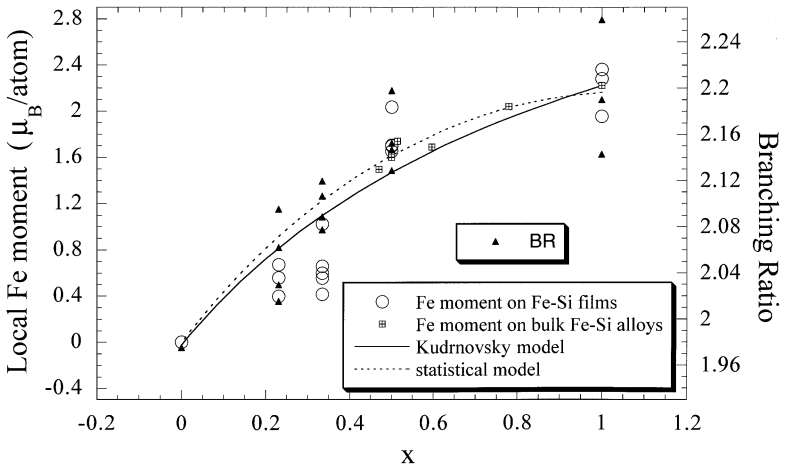


Fig. 5. Magnitude of the average Fe moment as a function of Fe concentration. The experimental XMCD data are indicated by open circles. The squares correspond to measurements performed on bulk Fe–Si alloys [1,14–16]. Solid and dashed lines correspond to two different models (see text). The triangles give the value of the branching ratio (BR) $I(L_3)/I(L_2)$.

magnitude of the Fe moment is concerned [12] Note that with this method we do not need to take into account the degree of polarization of the light. In fact similar results can be obtained by exploiting the sum rules given by Carra et al. [13]: the XMCD signal integrated over the $L_3$ peak is proportional to $3\langle L_z\rangle + 2\langle S_z\rangle$ (if the magnetic dipole operator $\langle T_z\rangle$ is not taken into account), which is, when $\mu_{\mathrm{orb}}$ is neglected, proportional to the magnetic moment $\mu(x)$.

The different values of $\mu(x)$ are plotted in Fig. 5 as a function of Fe concentration $x$. The multiple circles for each concentration represent several measurements on the same sample. We can see that the local magnetic moment depends strongly on $x$, and more precisely increases with increasing Fe concentration. Moreover, for FeSi the value of the moment is zero. Also presented in Fig. 5 by squares are the values measured by neutron scattering and saturation magnetization for bulk iron–silicon alloys [1,14–16]. These measurements give in $Fe_3Si$ a moment of 2.2–2.4 $\mu_B$ for the $Fe_I$ sites, and 1.2–1.35 $\mu_B$ for the $Fe_{II}$ sites. We can see that our data for the films are close to the mean Fe moment observed in bulk Fe–Si systems. Thus we tried to apply to our films the models used to describe the bulk Fe–Si alloys.

The first model (dashed line) has been proposed by Hines et al. [15]; the $Fe_I$ atoms, which are surrounded by eight $Fe_{II}$ atoms whatever the Fe concentration keep a local moment of 2.22 $\mu_B$, the same moment as bulk Fe. In other words, only the NN are taken into account, i.e. the $Fe_I$ atoms are screened by the $Fe_{II}$ atoms from an influence of the NNN. The $Fe_{II}$ atoms moment is deduced from Mössbauer and NMR measurements [17]. These data give the value of the hyperfine field at the $Fe_{II}$ site, which is found to depend only on the number of Fe NN (varying from 0 to 8), and not on the mean Fe concentration. Thus the magnitude of the $Fe_{II}$ moment depends only on the number of $Fe_I$ NN, at least for the stable bulk alloys investigated in Ref. [17], i.e. for $0.46 \leqslant x \leqslant 1$. Here we assume that this property is valid over the whole Fe concentration range, i.e. $0 \leqslant x \leqslant 1$. Hence the number of Fe NN for the various Fe concentrations are calculated by means of the binomial law:

$$P(i) = \frac{8!}{i!(8-i)!}x^i(1-x)^{(8-i)},$$

where $P(i)$ is the probability of finding $i$ $Fe_I$ NN for an $Fe_{II}$ atom in an $Fe(Si_{1-x}Fe_x)$ silicide. Moreover to obtain the value of the magnetic moment we

have considered that it scales with the measured hyperfine fields at the $Fe_{II}$ sites. Indeed it has been shown that the magnetization of Fe–Si alloys and the average internal magnetic field exhibit the same dependence as a function of Fe concentration [17]. One can see in Fig. 5 that the experimental data show a behavior that is rather properly described by the model. However for $Fe_2Si$ ($x = 0.33$) the magnetic moment is lower than the value given by this model.

A second model originates from ab initio calculations performed by Kudrnovsky et al. [14] in the frame of the so-called local environment model on Fe–Si alloys: the local magnetic moment has been calculated with the linear muffin-tin orbital method and the coherent potential approximation for the $Fe_{II}$ atoms and for $0.5 \leqslant x \leqslant 1$. In this approach the $Fe_{II}$ magnetic moment is found to depend linearly on the Fe concentration, ranging from pure Fe to $Fe_3Si$. In the present paper we extrapolate this linear dependence to lower Fe concentration (for $0 \leqslant x \leqslant 0.5$), as was done in Ref. [14]. In this way one obtains $\mu(Fe_{II}) = 0$ for FeSi, where the $Fe_{II}$ atoms are surrounded by eight Si atoms. This is in line with the Mössbauer measurements, where the hyperfine field is equal to zero when there are no Fe NN. In this local environment model, the moment of the $Fe_I$ atoms that are surrounded by eight $Fe_{II}$ atoms whatever the magnitude of $x$, remains at 2.22 $\mu_B$. One can see in Fig. 5 that this model gives values of $\mu(x)$ quite close to those of the statistical model, and that the experimental points exhibit the same trend. Again we note a tendency to observe lower moments than those predicted by this model for $x \leqslant 0.5$. Possibly this reflects merely the fact that our implicit assumption, that we essentially observe the magnetization at saturation $M(T = 0)$, is no longer a good approximation at RT in the films with $x \leqslant 0.5$ because of the decrease in Curie temperature and relevant finite temperature effects. In other words the mean temperature dependent magnetic moment associated with the ferromagnetic order measured by means of XMCD at RT is substantially lower than the local Fe moment.

Yet we can conclude that the local magnetic moment of the Fe atoms depends essentially on the chemical nature of the NN, rather than the magnitude of their moment. This also explains the fact that the Fe magnetic moment is similar for bulk $Fe_3Si$ and the $Fe_3Si$ films, although the $DO_3$ superstructure is not present in the $Fe_3Si$ films. This results are also in line with X-ray photoemission spectroscopy (XPS) measurements performed on these systems as discussed in Ref. [2]: the Fe2p and Fe3s core level signals presented multiplet splitting effects for the various silicide films grown on Si(1 1 1) except for FeSi, that were attributed to the presence of a local magnetic moment on the Fe atoms. However note that for $x = 0.09$ ($Fe_{1.2}Si$) XPS data seemed to indicate the presence of a magnetic moment on the Fe atoms, whereas no square hysteresis loop was observed with MOKE. Nevertheless, a saturation magnetization effect is observed in both $[\bar{1}\,0\,1]_{Si}$ and $[1\,\bar{2}\,1]_{Si}$ directions. Maybe the number of $Fe_I$ atoms is too low so that there is no remanence at all, at least at RT.

A further confirmation of the diminution of the local magnetic moment with Si content comes from the variation of the branching ratio $I(L_3)/I(L_2)$ in the absorption spectra with Fe concentration. $I(L_3)$ and $I(L_2)$ are the area under the $L_3$ and $L_2$ absorption peaks obtained from the half summation of the circularly polarized curves $(\sigma^+ + \sigma^-)/2$ which is, as pointed above, equivalent to the linear polarization absorption spectrum. The areas were estimated after subtraction of a linear background for each peak, by integrating the curves from 703.9 to 717.2 eV for $L_3$, and from 717.2 to 734.3 eV for $L_2$. The branching ratios (BR) obtained in this way are plotted in Fig. 5 with triangles. They decrease from 2.26 for pure Fe to 1.98 for FeSi. This last value is close to the statistical value of 2.00 [18], and has been already observed for non-magnetic Fe silicides [19]. This result confirms the fact that FeSi is not ferromagnetic and that no moment is carried by the Fe atoms. On the other hand, BR with a magnitude higher than the statistical value are attributed to high-spin states [18]. In other words, the BR reflects the behavior of the local magnetic moment. Note that a long-range ferromagnetic order is not necessary to observe the dependence of the branching ratio with the local magnetic moment. For example O'Brien et al. have shown that the BR for Mn in an ordered Cu(0 0 1)c(2$x$2)Mn

surface alloy phase is higher than for bulk-like epitaxial Mn on Cu(0 0 1), thus indicating a higher local magnetic moment for Mn within the alloy [20]. However no long range ferromagnetic order was detected for both systems. We can see in Fig. 5 that the BR decreases versus $x$ in a way similar to that of the magnetic moment. A decrease of the iron magnetic moment with decreasing Fe concentration accompanied by a reduction of the BR has been already observed on Fe–Ge amorphous alloys [21]. Concerning this moment diminution, it has been suggested that in the Fe–Si alloys d-like electrons are transferred from Si to Fe, thus reducing the number of d-holes and in turn the magnitude of the moment [17]. However, Morrison et al. have shown that for $Fe_xGe_{1-x}$ amorphous alloys the number of holes does not depend on $x$ [21]. In contrast, they suggest that the reduction of the magnetic moment is rather due to hybridization causing modifications in spin pairing.

## 4. Summary

In conclusion, we have shown that iron silicides $Fe(Si_{1-x}Fe_x)$ films with a thickness of $\sim 200$ Å are ferromagnetic at RT on the whole range of concentration $0.15 \leqslant x \leqslant 1$. The magnetic anisotropy is uniaxial, with the easy axis lying along a $[\bar{1}\,0\,1]_{Si}$ crystallographic direction, and the hard axis along a $[1\,\bar{2}\,1]_{Si}$ direction. The average magnetic moment on the Fe atoms decreases with increasing Si concentration. This reduction is attributed to the diminution of the total number of $Fe_I$ atoms, and to the reduction of the $Fe_{II}$ magnetic moment upon increasing the number of Si NN.

## References

[1] V. Niculescu, J.I. Budnick, Solid State Commun. 24 (1977) 631.
[2] S. Hong, P. Wetzel, G. Gewinner, D. Bolmont, C. Pirri, J. Appl. Phys. 78 (1995) 5404.
[3] M. Fallot, Ann. Phys. 6 (1936) 305.
[4] S. Hong, C. Pirri, P. Wetzel, D. Bolmont, G. Gewinner, S. Boukari, E. Beaurepaire, J. Magn. Magn. Mater. 165 (1997) 212.
[5] C. Pirri, M.H. Tuilier, P. Wetzel, S. Hong, D. Bolmont, G. Gewinner, R. Cortès, O. Heckmann, H. von Känel, Phys. Rev. B 51 (1995) 2302.
[6] H. von Känel, K.A. Mäder, E. Müller, N. Onda, H. Sirringhaus, Phys. Rev. B 45 (1992) 13807.
[7] S. Hong, Ph.D. Thesis, unpublished
[8] J.A.C. Bland, M.J. Baird, H.T. Leung, A.J.R. Ives, K.D. Mackay, H.P. Hughes, J. Magn. Magn. Mater. 113 (1992) 178.
[9] E. Kneller, Ferromagnetismus, Springer, Berlin, 1962, p. 536.
[10] W.L. O'Brien, B.P. Tonner, Phys. Rev. B 50 (1994) 2963.
[11] M. Alouani, J.M. Wills, J.W. Wilkins, Phys. Rev. B 57 (1998) 9502.
[12] G.W. Anderson, M.C. Hanf, P.R. Norton, M. Kowalewski, K. Myrtle, B. Heinrich, J. Appl. Phys. 79 (1996) 4954.
[13] Paolo Carra, B.T. Thole, Massimo Altarelli, Xindong Wang, Phys. Rev. Lett. 70 (1993) 694.
[14] J. Kudrnovsky, N.E. Christensen, O.K. Andersen, Phys. Rev. B 43 (1991) 5924.
[15] W.A. Hines, A.H. Menotti, J.I. Budnick, T.J. Burch, T. Litrenta, V. Niculescu, K. Raj, Phys. Rev. B 13 (1976) 4060.
[16] J. Moss, P.J. Brown, J. Phys. F: Metal Phys. 2 (1972) 358.
[17] M.B. Stearns, Phys. Rev. 129 (1963) 1136.
[18] B.T. Thole, G. van der Laan, Phys. Rev. B 38 (1988) 3158.
[19] Fausto Sirotti, Maurizio De Santis, Giorgio Rossi, Phys. Rev. B 48 (1993) 8299.
[20] W.L. O'Brien, J. Zhang, B.P. Tonner, J. Phys.: Condens. Matter 5 (1993) L515.
[21] T.I. Morrison, M.B. Brodsky, N.J. Zaluzec, Phys. Rev. B 32 (1985) 3107.
[22] J.J. Krebs, B.T. Jonker, G.A. Prinz, J. Appl. Phys. 61 (1987) 2596.